Waggoner, A. (1976), in The Enzymes of Biological Membranes, Martonosi, A., Ed., New York, N.Y., Plenum Press, p 119.

Yguerabide, J. (1972), *Methods Enzymol. 26,* 498.

Yip, K. L., Lipari, N. O., Duke, C. B., Hudson, B., and Diamond, J. (1976), *J. Chem. Phys. 64,* 4020.

Conjugated Polyene Fatty Acids as Fluorescent Probes: Synthetic Phospholipid Membrane Studies†

Larry A. Sklar,‡ Bruce S. Hudson,*,§ and Robert D. Simoni¶

ABSTRACT: The preparation of polyene fatty acid membrane probes *cis*- and *trans*-parinaric acid and parinaroylphosphatidylcholines and their use in studies of several one- and two-component lipid systems are described. The fluorescence quantum yield of *trans*-parinaric acid in dipalmitoylphosphatidylcholine at 20 °C is approximately 0.3; the quantum yield in aqueous solution is negligibly small. Thermal-phase transitions in single-component phospholipid dispersions are monitored with absorption and fluorescence excitation peak position, fluorescence intensity, lifetime, and polarization. The transition temperatures observed are consistent with previous determinations. Shifts in the absorption peak position are related to the bilayer expansion as it undergoes the gel to liquid-crystalline transition, while fluorescence depolarization provides semiquantitative information concerning molecular motion of the probe in the bilayer. A long fluorescence lifetime component is observed for parinaric acid in the solid phase (up to 50 ns), and a short lifetime component is observed (ca. 5 ns) in the fluid phase of dipalmitoylphosphatidylcholine; both lifetime components are observed in the transition region. In most phospholipids, *cis*-parinaric acid detects the melting transition at about 1 °C lower than *trans*-parinaric acid. Partitioning experiments involving mixed populations of phospholipid vesicles show that *trans*-parinaric acid preferentially associates with solid-phase lipids, while *cis*-parinaric acid shows a more equal distribution between solid and fluid lipids. The binding of *cis*-parinaric acid to dipalmitoylphosphatidylcholine at 25 °C is described as a partitioning of parinaric acid between lipid vesicles and the aqueous phase with a partition coefficient of 5×10^5. Several rates are observed in the binding process which are interpreted as rapid outer monolayer uptake and a much slower process of interlamellar exchange. The phase diagram of the binary lipid mixture dipalmitoylphosphatidylcholine–dipalmitoylphosphatidylethanolamine has also been examined and found to be essentially identical to the one constructed using a nitroxide probe.

In the previous paper of this issue (Sklar et al., 1977), the spectral properties of the isomers of the linear polyene fatty acid, parinaric acid, were described. In this paper, the preparation of these probes (I, II, and III) and their spectral properties in model lipid systems are described. The behavior of various spectral parameters of the probes is related to the considerable wealth of information about bilayer structures derived from other techniques.

Materials and Methods

Polyene Fatty Acids. Parinaric acid (9,11,13,15-octadecatetraeneoic acid, PnA[1]; commercially available from Molecular Probes, Roseville, Minn.) was first isolated in 1933 from *Parinari laurinum*[2] (Eckey, 1954). The seed kernel is about 15% oil and nearly 60% of the fatty acid component is parinaric acid (Riley, 1950). About 3 g of PnA can be obtained from a single seed using the procedure described below. The natural product (I), known as α-parinaric acid, was identified as the cis,trans,trans,cis isomer by Gunstone and Subbarao (1967). β-Parinaric acid (II) obtained by treatment of α-parinaric acid with iodine has the all-trans configuration

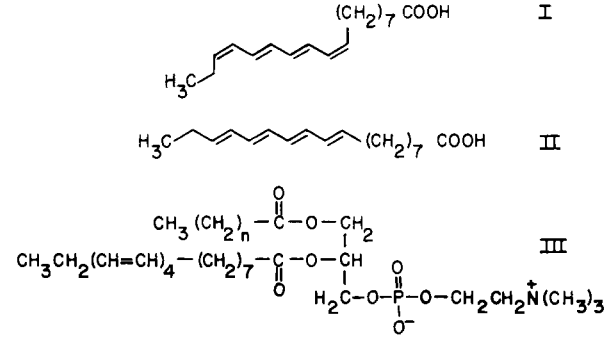

† From the Departments of Chemistry and Biological Sciences, Stanford University, Stanford, California 94305. *Received July 13, 1976.* This work was supported by the National Institutes of Health (Grants GM21149 and EY01518 to B.S.H. and GM18539 to R.D.S.) and a grant from the Research Corporation to B.S.H.

‡ Taken in part from the thesis submitted by L.A.S. in partial fulfillment of the Ph.D. requirements, Stanford University (1976). Present address: Natural Sciences II, University of California, Santa Cruz, Santa Cruz, Calif. 95064.

§ Camille and Henry Dreyfus Teacher-Scholar and Alfred P. Sloan Fellow.

¶ Department of Biological Sciences, Stanford University.

[1] Abbreviations used are: DMPC, dimyristoylphosphatidylcholine; DPPC, dipalmitoylphosphatidylcholine; DSPC, distearoylphosphatidylcholine; DPPE, dipalmitoylphosphatidylethanolamine; BHT, 2,6-di-*tert*-butyl-4-methylphenol; PnA, parinaric acid; *cis*-PnA, α-parinaric acid; *trans*-PnA, β-parinaric acid; Me_2DPPE, *N,N*-dimethyl-DPPE; Tempo, 2,2,6,6-tetramethylpiperidinyl-1-oxy; TLC, thin-layer chromatography; IR, infrared; UV, ultraviolet.

[2] Most references use the species name *Parinarium laurinum* (Riley, 1950, Gunstone and Subbarao, 1967). According to the botanical literature this is equivalent to *Parinarium glaberrimum* (Kramer, 1951) and the modern name is *Parinari glaberrimum* (Backer and Bakhuizen Van den Brink, 1963). For general reviews of the occurrence and chemistry of fatty acids with conjugated unsaturation, see Hopkins (1972) and Solodovnik (1967).

(Kaufmann and Sud, 1959). We will refer to these isomers as *cis*- and *trans*-PnA, respectively.

Seeds of the plant *Parinari glaberrimum* were obtained through the assistance of R. H. Phillips of the Nasese Nursery, Suva, Fiji. The seeds are stored in sealed containers at −20 °C. Seed kernels were ground with mortar and pestle. The oils were extracted from 215 g of kernel with 8 volumes, 250 mL each, of anhydrous diethyl ether with further grinding. BHT (2,6-di-*tert*-butyl-4-methylphenol, NBC Biochemicals) was added to the ether in amounts of 1 mg/100 mL as antioxidant. The extract was gently flash evaporated without heating, yielding 32 g of light yellow oil, or 15% of the kernel by weight. The oil was saponified in 300 mL of fresh 5% methanolic KOH under an atmosphere of argon with gentle refluxing and stirring for 30 min. The solution was brown in color. The hot reaction mixture was acidified with 125 mL of 2 M HCl, and the free fatty acids were extracted in a minimal amount of refluxing petroleum ether (boiling range 30–60 °C), producing a pale yellow solution. White crystals grow rapidly when the petroleum ether extract is cooled to 5 °C. *cis*-PnA is purified by repeated recrystallization from petroleum ether. After five recrystallizations, the compositions of the mother liquor and the product crystals are identical. Ten grams of white crystalline plates (melting point 84–85 °C) is obtained from 32 g of oil. Gas chromatography of the methyl esters shows a trace of eleostearic acid (ca. 1%) along with the natural product tetraene, *cis*-PnA.

trans-PnA was prepared from *cis*-PnA as follows. Freshly recrystallized *cis*-PnA (6 g), without BHT,[3] was dissolved under argon in a minimal amount of refluxing hexane. Fifty microliters of hexane saturated with iodine is added to the hot hexane solution and exposed to direct sunlight for 10 min, or until the solution begins to become cloudy. As the hexane cools, small crystals of *trans*-PnA appear. Crystals form rapidly when the solution is plunged into an ice bath. The unconverted *cis*-PnA remains in solution. The *trans*-isomer is recrystallized from hexane requiring 10 to 20 mL of hexane (containing 1 mg of BHT) for each gram of *trans*-PnA. Gas chromatographic analyses of mother liquor and crystals are identical after three recrystallizations and show no cis isomer and only a trace of triene. Four grams of *trans*-PnA are obtained from 6 g of *cis*-PnA. The trans isomer forms white needle-like crystals with melting point 95–96 °C.

Storage of Polyene Fatty Acids. PnA can be stored under the recrystallization solvent or ethanol containing BHT and an argon atmosphere at −20 °C. Over periods of months, a small amount of yellowed material, which does not completely dissolve, may appear in these samples. Standard solutions, in ethanol, prepared from freshly recrystallized material and containing 1 mg/mL of *cis*-PnA or 0.5 mg/mL of *trans*-PnA are stable for indefinite periods when stored under argon, in darkness, with small amounts of BHT at −20 °C and are used for addition to aqueous solution.

Analytical Methods. The purity of our materials compares favorably with that obtained by other researchers on the basis of gas chromatography, the sharpness of the absorption peaks (indicating isomeric purity), the extinction coefficients, and the absence of triene absorption in the 250-nm region (Riley, 1950; Kaufman and Sud, 1959; Gunstone and Subbarao, 1967). Our melting points are sharp and at temperatures equal to or above those reported by other workers.

[3] BHT must be removed by recrystallization of *cis*-PnA from petroleum ether because it appears to inhibit the action of iodine in the isomerization, presumably by acting as a free-radical trap.

Methyl esters of the fatty acids were prepared with dimethylformamide dimethyl acetal (Methyl-8 from Supelco) or with diazomethane. Analytical separations were performed on an F&M, Model 700, gas chromatograph equipped with a flame-ionization detector. Good separations were obtained with two types of gas chromatography columns. A 6 ft × ⅛ in. column containing 20% diethylene glycol succinate (DEGS) on 80/100 Chromosorb W at 210 °C provides resolution of all the fatty acid components. Separation of *cis*- and *trans*-PnA can be obtained with a 3 ft × ⅛ in. column containing 10% SP 2340 on 100/120 Supelcoport at 180 °C. On the SP 2340 column, the carbon number for the two isomers is about 27.2 and 27.7 for cis and trans, respectively.

Synthetic Procedures. Phospholipids (dimyristoylphosphatidylcholine (DMPC), dipalmitoylphosphatidylcholine (DPPC), distearoylphosphatidylcholine (DSPC), *N,N*-dimethyldipalmitoylphosphatidylethanolamine (Me_2 DPPE), and dipalmitoylphosphatidylethanolamine (DPPE)) were obtained from Calbiochem. Thin-layer chromatography of these lipids indicated a high degree of purity and they were used without further purification. Fatty acids were obtained as follows: myristic, Aldrich, 99.5%; palmitic, Sigma, 99+%; stearic, Chemical Samples Co., 99.5%. Phospholipase A_2 was obtained as the lyophilized venom of *Crotalus adamanteus* from the Miami Serpentarium Laboratories. All solvents and reagents were obtained from commercial sources and were of the highest purity commercially available.

Phoshatidylcholines containing *cis*-PnA in the 2 position were prepared by a modification of the procedure of Robles and Van Den Berg (1969). Lysophosphatidylcholines were prepared by the action of phospholipase A_2 on phosphatidylcholine (Hanahan, 1952; Hubbell and McConnell, 1971). The synthesis of 1-stearoyl-2-*cis*-parinaroylphosphatidylcholine from lyso-1-stearoyl-phosphatidylcholine is outlined.

Parinaroyl-mixed anhydrides were prepared as follows: 257 mg (0.90 mmol) of stearic acid and 28 mg of *cis*-PnA (0.10 mmol) were dissolved in 75 ml of CCl_4 to which was added 103 mg (0.05 mmol) of dicyclohexylcarbodiimide (DCCD) dissolved in 25 mL of CCl_4. The mixture was stirred under argon at room temperature for 12 h. The dicyclohexylurea and any polymerized insoluble material from the polyene were filtered from the reaction mixture, and the anhydride (in CCl_4) was identified by IR peaks at 1815 and 1750 cm^{-1}. Ultraviolet analysis of the anhydride indicated it contained 0.08 mmol of PnA. The acylation conditions differ in several important aspects from the conditions described by Robles and Van Den Berg (1969). We had difficulty in preparing the sodium salt of *cis*-PnA and substituted the salt of the saturated fatty acid; the use of pure PnA anhydride results in a polymerized product. Dry sodium stearate (0.2 mmol) and dry stearoyllysophosphatidylcholine (0.067 mmol) were added to a 10-mL pear-shaped flask. The anhydride solution was reduced in volume, added to the flask, and flash evaporated. Glass beads were added and the flask was sealed and evacuated for 24 h in darkness at room temperature. The flask was rotated and heated to 75 °C for 6 h. Thin-layer chromatography of the product, using Silica Gel S/UV254 (Macherey, Nagel & Co., Germany) developed in 65 mL of $CHCl_3$–25 mL of MeOH–5 mL of water, according to the method of Peifer (1962), indicated that the reaction was essentially complete. Mineral lamp illumination of the TLC plate revealed blue emission from the PnA-containing spots; emission in the phosphatidylcholine spot was observed. The reaction product (III, $n = 16$) was dissolved in 3 mL of 10% methanol in chloroform, filtered, and purified on a column containing 10 g of freshly activated silicic acid by

elution with graded chloroform–methanol mixtures. The product, obtained at 20–35% methanol, exhibited a single TLC spot. The yield was determined by phosphate analysis by the method of Bartlett (1959) and UV characterization of the product. The product solution was very slightly yellow. The yield was 0.018 mmol (14 mg) of mixed lecithin, or 25% based on the lysolecithin. The ultraviolet absorption was nearly identical to the starting PnA, except that slight peak broadening and a 1-nm (blue) shift probably indicate the presence of a small fraction of trans isomer (10%), and slightly increased absorption in the 250- to 280-nm region indicates the appearance of trienoic material. It was calculated from the optical density of the product and the phosphate determinations that 7% of the lecithin molecules contained acylated parinaric acid. We have assumed the remaining 93% is DSPC, the 7% being 1-stearoyl-2-parinaroylphosphatidylcholine. The composition of the resulting phospholipid is similar to the composition of the mixed anhydride. These reactions were repeated with DMPC and DPPC (at 65 and 70 °C, respectively), using mixed anhydrides containing 2 to 10% PnA, and the products had composition similar to that of the mixed anhydride. Phospholipids containing PnA have also been prepared from the acid chloride using the method of Baer and Buchnea (1959).

The action of phospholipase A_2 from *Crotalus adamanteus* on the parinaroyl derivative of DMPC was followed by the fluorescence of PnA-containing spots on TLC. The starting material, a mixture of DMPC and 1-myristoyl-2-parinoylphosphatidylcholine, shows fluorscence in a TLC spot identified as PC by comparison to a pure DMPC standard by iodine staining. The action of phospholipase on this material produces a lysolecithin and fatty acid spot visualized by iodine staining. Only the fatty acid spot can be visualized by fluorescence. We conclude that the enzyme is active upon phospholipids containing PnA in the 2 position, and that the synthetic phospholipids contain PnA in only the 2 position.

Lipid Dispersions. Phospholipids, dried from chloroform, were dispersed in 0.01 M, pH 7.4, potassium phosphate buffer, by vortexing for 30 s above the transition temperature of the lipid. PnA was usually added after dispersion to samples above their transition temperature which had been vigorously deoxygenated with argon. Occasionally, PnA was added to the buffer prior to dispersion, in concentrations never exceeding 10^{-6} M, and samples were dispersed under argon. In some experiments, BHT was added as antioxidant, but never in excess of 1 BHT/100 phospholipid molecules. The final concentration of lipid for each experiment is specified in the figure legends.

Spectroscopy. Absorption spectra were recorded on a Cary 14 scanning spectrophotometer. Fluorescence measurements were recorded on an Hitachi Perkin-Elmer MPF-2A fluorimeter attached to a Mosely 7030A X–Y recorder. In measurements of lipid-phase transitions, the sample temperature was monitored by a copper–constantan thermocouple inside a jacketed cuvette, and the output of the thermocouple was used to drive the x axis of the recorder. The fluorimeter output, scaled by a Keithly-621 electrometer, was used to drive the y axis. Sample temperature was controlled by a circulating water bath, and the rate of temperature variation never exceeded 2 °C/minute. The samples were deoxygenated with argon. Temperature variation was usually decreasing and then increasing in temperature, sometimes with multiple scans. Peak positions of excitation spectra were estimated to the nearest 0.1 nm, and repetitive determinations indicate a reproducibility of 0.3 nm. The peak positions were calibrated with emission lines from a low-pressure mercury lamp. In some cases, phase-transition curves were generated with computer assistance in which case the X–Y recorder curves of phospholipid-phase transitions were traced manually on a Calma, Model 302, Digitizer.

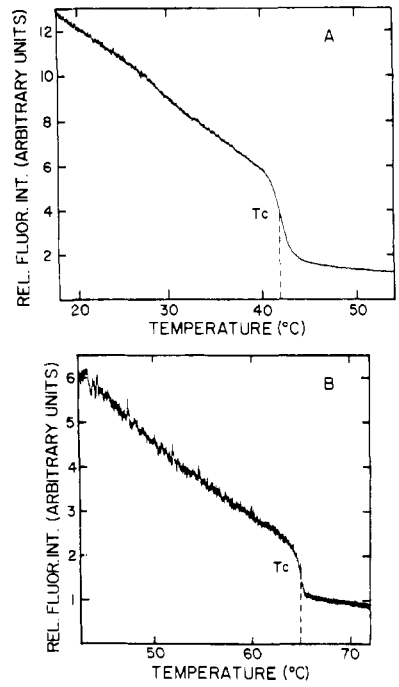

FIGURE 1: The fluorescence intensity of *trans*-PnA in DPPC (A) and DPPE (B) dispersions as a function of temperature. The experimental conditions are given in the legend to Figure 4. Curve 2 of Figure 4A is the replotted version of A and curve 5 corresponds to B.

Results and Discussion

Lipid-Phase Transitions Detected by the Fluorescence Intensity of Parinaric Acid. Figure 1 shows the response of the fluorescence intensity of *trans*-PnA to the gel to liquid-crystalline phase transition of aqueous dispersions of DPPC (A) and DPPE (B). The data are the direct output from the X–Y plotter. The y axis has been expanded twofold for the DPPE data. The temperature at the midpoint of the transition will be referred to as T_c. The quantum yield for *trans*-PnA in DPPC at 20 °C is approximately 0.3.

The fluorescence intensity of a sample of DPPC containing *trans*-PnA is plotted against temperature in Figure 2A. The main melting transition occurs at 42.5 °C and has a width of about 1.5 °C. A pretransition is observed in the temperature range of 32–37 °C in the initial heating. When the sample is heated and cooled at the rate of 0.5 °C/minute no hysteresis is observed in the main transition; however, hysteresis is apparent in the pretransition. The magnitude of the pretransition and the temperature at which it occurs seem dependent upon the history of the sample and the rate at which temperature is varied in the course of the experiment.

The fluorescence data of Figure 2A have been plotted on a logarithmic scale vs. the reciprocal of temperature (K^{-1}) in Figure 2B. The rational for this presentation is given in Sklar et al. (1977): when the fluorescence intensity of a solution of PnA is plotted as the logarithm of intensity vs. $1/T$, a linear relationship is obtained with a characteristic slope θ.

Several parameters which describe phospholipid-phase transitions detected by the response of the fluorescence intensity of PnA are defined in Figure 2B. The slope θ_f represents the temperature dependence of the fluorescence intensity of

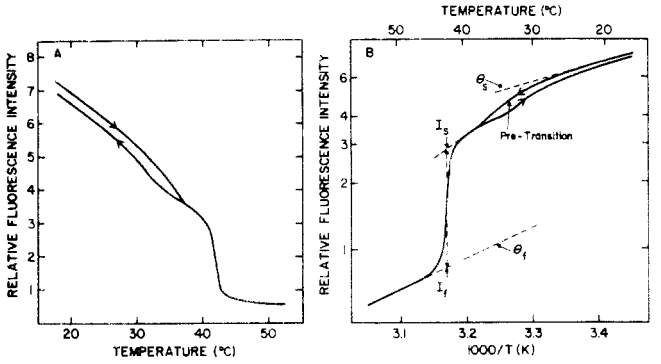

FIGURE 2: Response of the fluorescence intensity of *trans*-PnA to the thermal-phase transition of a DPPC dispersion. (A) I vs. T; (B) log vs. $1/T$. The lipid dispersion (0.05 mg/mL, 6.6×10^{-5} M) was prepared in 0.01 M, pH 7.4, phosphate buffer. *trans*-PnA was added at 50 °C (2.6×10^{-7} M, ratio of 1 probe per 250 lipid molecules) and and the temperature was reduced to 15 °C. The sample was deoxygenated with argon continuously during the fluorescence measurements. Excitation was at 320 nm (2 nm slit) and emission at 410 nm (20 nm slit). Data were collected as the sample was heated from 15 to 55 °C, then cooled, at the rate of 0.5 °C/minute.

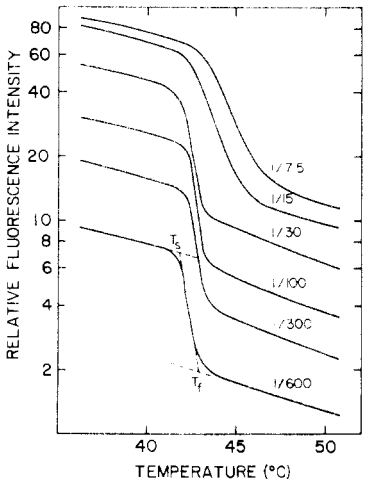

FIGURE 3: Temperature scans of the *trans*-PnA fluorescence intensity (on a logarithmic scale) vs. T for different probe/lipid ratios in a DPPC dispersion. The lipid dispersion was prepared as in Figure 2. *trans*-PnA was added in probe/lipid ratios varying from $1/600$ to $1/7.5$, at 50 °C, and equilibrated for 10 min during which it was deoxygenated with argon. The sample was cooled to 35 °C, and then heated to 50 °C at the rate of 0.5 °C/min, employing the fluorescence conditions described in Figure 2.

PnA in fluid-phase lipids and is defined as the range, in K^{-1}, over which the fluorescence intensity doubles. The slope θ_s is the solid-phase temperature dependence (at temperatures below the pretransition for lipids in which the pretransition is observed). θ_f is typically in the range of 2.2×10^{-4} K^{-1}, which is comparable to the values observed for *cis*- and *trans*-PnA in solution (Sklar et al., 1977). The magnitude of the transition I_s/I_f is defined in terms of the intercepts shown in Figure 2B. The intensity at the midpoint of the transition, I_c, is picked so that $(I_c - I_f)/(I_s - I_f) = 0.5$.

The effect of varying the amount of probe on the phase transition detected in DPPC is shown in Figure 3. The probe concentration has been varied (at constant lipid concentration) from 1 *trans*-PnA added per 600 phospholipid molecules to 1 per 7.5. The temperature, magnitude, and width ($T_f - T_s$, Figure 4) of the transition are virtually unaffected by the increase in the ratio of *trans*-PnA added up to 1/30. The most pronounced changes occur above this level, so that at 1/7.5 the

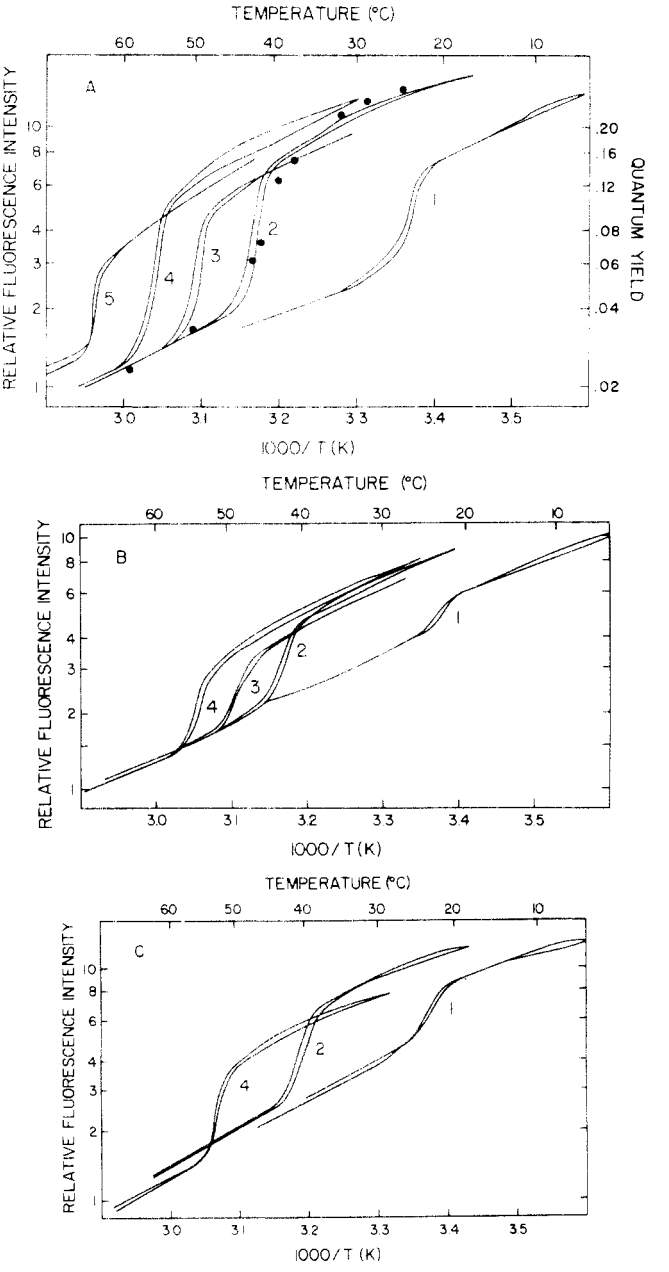

FIGURE 4: The response of the fluorescence intensity of parinaric acid probes to the thermal-phase transitions of several phospholipids. (A) *trans*-PnA, (B) *cis*-PnA, (C) 1-acyl-2-*cis*-parinaroylphosphatidylcholine. The lipids are designated as follows: (1) DMPC, (2) DPPC, (3) Me_2DPPE, (4) DSPC, and (5) DPPE. In each case, 0.2 mg of lipid (approximately 2.5×10^{-7} mol) was deposited by evaporation of a chloroform solution containing 2×10^{-9} mol of BHT. In A, the lipids were dispersed under argon by vortexing 15 °C above the lipid-phase transition temperature in 4.0 mL of freshly prepared solution of *trans*-PnA (1.9×10^{-7} M) in 0.01 M, pH 7.4, phosphate buffer. The probe/lipid ratio was approximately $1/350$. Each sample was cooled to about 15 °C below the lipid-transition temperature and then heated at a rate not exceeding 2 °C/minute. This heating curve and a subsequent cooling curve are shown in each case. Fluorescence measurements used excitation at 320 nm (1.5 nm slit) and emission at 410 nm (30 nm slit). The solid circles (●) for curve 2 are calculated from the data of Figure 5 from eq 2, as described in the text, and scaled to a quantum yield of 0.3 at 20 °C. In B, the concentration of *cis*-PnA in buffer was 2.2×10^{-7} M (a probe/lipid ratio of approximately $1/300$) and fluorescence excitation was at 325 nm (1.5-nm slit). In C, the synthetic parinaroyl phospholipids were added to the chloroform solution and dried down. The probe to unlabeled lipid ratio was $1/200$. The lipids were dispersed in phosphate buffer. Fluorescence excitation was at 324 nm (1.5-nm slit) and emission was at 410 nm (24-nm slit). For 1 (DMPC) the probe is 1-myristoyl-2-*cis*-parinaroylphosphatidylcholine, for 2 (DPPC) it is 1-palmitoyl-2-*cis*-parinaroylphosphotidylcholine, and for 4 (DSPC) it is 1-stearoyl-2-*cis*-parinaroylphosphatidylcholine.

TABLE I: Phase-Transision Parameters for Polyene Probes in Phospholipid Dispersions.

Lipid	Probe	T_c[a] (°C)	T_p[a] (°C)	θ_f ($10^{-4}K^{-1}$)	θ_s ($10^{-4}K^{-1}$)	I_s/I_f
DMPC	*trans*-PnA	24.0	11	2.6	>2.5	2.3
DMPC	*cis*-PnA	23.0	10	2.2	~3.0	1.3
DMPC	MPnPC[b]	23.0	8	1.9	>3.0	1.6
DPPC	*trans*-PnA	42.5	32	2.2	~3.0	3.3
DPPC	*cis*-PnA	42.0	32	2.3	3.0	2.0
DPPC	PPnPC[b]	40.5	~30	1.9	>3.0	2.2
Me_2DPPE[c]	*trans*-PnA	50.0		2.2	2.5	2.7
Me_2DPPE[c]	*cis*-PnA	49.0		2.1	2.7	1.7
DSPC	*trans*-PnA	55.0	48	2.2	2.5	3.4
DSPC	*cis*-PnA	54.0	49	2.3	2.7	2.1
DSPC	SPnPC[b]	53.5	47	2.0	>3.0	2.2
DPPE	*trans*-PnA	64.5		2.5	~2.0	2.1
DPPE	*cis*-PnA	64.0		~2.0	~2.0	1.4

[a] Pretransition temperature. [b] MPnPC, 1-myristoyl-2-parinaroylphosphatidylcholine; PPnPC, 1-palmitoyl-2-parinaroylphosphatidylcholine; SPnPC, 1-stearoyl-2-parinaroylphosphatidylcholine. [c] Me_2DPPE, *N,N*-dimethyldipalmitoylphosphatidylethanolamine.

width has increased from 1.5° to 4°, the temperature from 43 to 45 °C, and the magnitude from 3.5 to 4.0.

Transitions have been measured for dispersions of several phospholipids using *cis*- and *trans*-PnA and the *cis*-PnA phospholipid derivatives. These results are shown in Figure 4, and the phase-transition parameters are summarized in Table I. Our transition temperatures agree quite well with those determined by other methods (Shimshick and McConnell, 1973; Hinz and Sturtevant, 1972). The calorimetric values are 23.70 °C (DMPC), 41.75 °C (DPPC), and 54.24 °C (DSPC), while the nitroxide probe values are 23.2 °C (DMPC), 40.5 °C (DPPC), 54.0 °C (DSPC), and 63.0 °C (DPPE). The width of these transitions, 1–2°, is as narrow as that reported with any fluorescent probe (Jacobson and Papahadjopoulos, 1975), and comparable to those reported using calorimetry or electron spin resonance probes.

Several trends in the data presented in Table I are noteworthy. In general, the transition temperature detected by the phospholipid probe is lower than that detected by *cis*-PnA, which is lower than that detected by *trans*-PnA. The transition magnitude, I_s/I_f, is larger for *trans*-PnA than for *cis*-PnA by a factor of about 1.6. The transition magnitude is essentially identical for DSPC and DPPC, but somewhat smaller for DMPC. The fluid-phase value of the fluorescence intensity (Figure 4) is similar in these phosphatidylcholines but the solid-phase fluorescence intensity is lower in DMPC than either DPPC or DSPC.

The similarity of parameters of the phase transitions detected by *cis*-PnA and by the phospholipid derivative of *cis*-parinaric acid (Table I) is strong evidence that the fatty acid probe remains dissolved in the lipid both above and below the phase transition. Therefore, the reduction of the fluorescence intensity in response to the phase transition reflects changes in the physical structure of the lipids, rather than exclusion of the probe from the lipid phase as it melts.

Fluorescence Lifetimes of Parinaric Acid in DPPC Dispersions. The fluorescence lifetimes of both *cis*- and *trans*-PnA in DPPC dispersions were studied as a function of temperature. Below the DPPC transition temperature, the fluorescence decay can be fitted with a single lifetime; however, near the transition temperature a double exponential decay is observed. Data were therefore fitted with two lifetime components and the results are presented in Figure 5 as plots of fluorescence

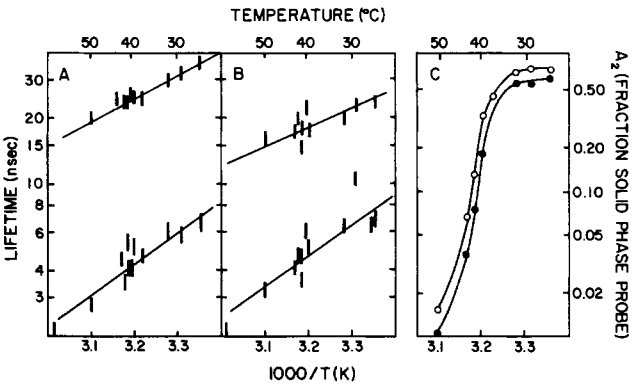

FIGURE 5: The response of the fluorescence lifetimes of PnA probes to the thermal transition of a DPPC dispersion. (A and B) Log (τ) vs. $1/T$ for *trans*- and *cis*-PnA. (C) The variation in the fraction of the long-time component (A_2) for *cis*- (filled circles) and *trans*- (open circles) PnA in DPPC. The lipid dispersions contained 0.05 mg/mL DPPC, 1 BHT/400 DPPC, and 1 PnA/35 DPPC in 0.01 M, pH 7.4, phosphate buffer. The fluorescence excitation pulse was filtered by a Corning 7-54 (9863) UV band-pass filter and the emission was filtered by a Corning 3-74 (3391) sharp-cut filter. The sample temperature was monitored by a thermometer in an identical cuvette and was controlled by a circulating water bath. At least 30 min equilibration time was allowed at each temperature. For each measurement, the lamp pulse was determined by recording the signal scattered from polystyrene spheres. A lipid-scattering blank was monitored for the same length of time as the sample. The blank signal was only a few percent of the fluorescence signal.

lifetime (on a logarithmic scale) vs. K^{-1}. In Figure 5A, B, it is seen that the individual long and short components have values which are temperature dependent.

The temperature dependence of the fluorescence lifetime can be characterized by slopes θ_s^τ and θ_f^τ given by the slopes of the lines as shown in Figure 5A, B. These values for solid and fluid phase are 3.6×10^{-4} K^{-1} and 2.2×10^{-4} K^{-1} for *cis*-PnA and 3.0×10^{-4} K^{-1} and 2.1×10^{-4} K^{-1} for *trans*-PnA, which correspond quite well to the θ values obtained for the fluorescence intensity, as shown in Table I. The agreement substantiates the result from solvent studies that changes in fluorescence quantum yield are produced by lifetime changes; i.e., the primary effect is a temperature dependent nonradiative process. The radiative rate, k_e, is roughly constant.

The time dependence of the fluorescence intensity after an

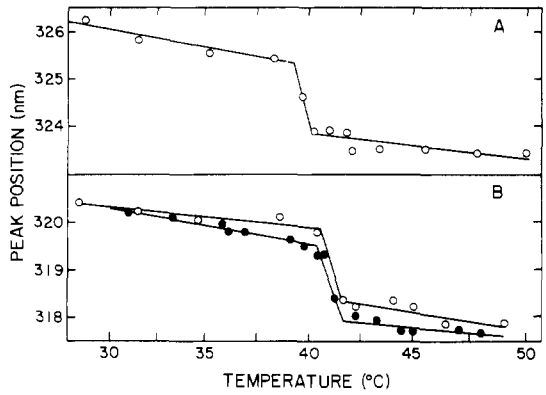

FIGURE 6: The excitation peak position of (A) *cis*- and (B) *trans*-PnA in DPPC vesicles as a function of temperature. DPPC dispersions (0.05 mg/mL) containing 1 BHT/150 DPPC and 1 PnA/30 DPPC were prepared in 0.01 M, pH 7.4, phosphate buffer. Excitation spectra were recorded as the sample was cooled from 50 to 20 °C with an excitation slit of 2 nm and an emission slit of 30 nm centered at 410 nm. The absorption peak positions for *trans*-PnA in DPPC were also determined (filled circles in B). A dispersion of 0.10 mg/mL DPPC containing 1 BHT/20 DPPC and 1 *trans*-PnA/20 DPPC was prepared in 0.01 M, pH 7.5, phosphate buffer. Multiple determinations indicate that absorption peaks could be reproducibly measured to 0.2 nm.

exciting pulse is given by eq 1 when the lamp pulse has been deconvoluted.

$$I(t)/I(0) = A_1 e^{-t/\tau_1} + A_2 e^{-t/\tau_2} \quad (1)$$

$\tau_2 > \tau_1$ by definition and $A_1 + A_2 = 1$. A_2 represents the fraction of long lifetime fluorescence. The temperature dependence of A_2 is shown in Figure 5C. The fraction of long lifetime fluorescence decreases abruptly at the phase-transition temperature of 41 °C. The long lifetime component is therefore identified with the probe in the solid phase.

A relative preference of *trans*-PnA for the solid phase, as compared to *cis*-PnA, is apparent from Figure 5C. Since the magnitude of A_2 is related to the fraction of probe molecules in the solid phase, the observation that A_2 for *trans*-PnA (open circles) is significantly greater than for *cis*-PnA (filled circles) at temperatures within the transition region implies that the trans probe has a relative preference for solid region; this result is consistent with the higher T_c's detected by *trans*-PnA in Table I.

A comparison of the temperature dependence of the fluorescence intensity of *trans*-PnA in DPPC with that expected based on the lifetime measurements is shown in Figure 4A (points). Integration of eq 1 leads to the expression

$$Q = \bar{k}_c \bar{\tau} = \bar{k}_c (A_1 \tau_1 + A_2 \tau_2) \quad (2)$$

where Q is the fluorescence quantum yield, $\bar{k}_c$ is an average radiative rate constant, and $\bar{\tau}$ is the average lifetime ($A_1\tau_1 + A_2\tau_2$). This simple form results from the fact that the radiative rate constant for this probe is essentially independent of environment (Sklar et al., 1977). The values for solid and fluid lipid phases may therefore be equated to their average and factored as in eq 2. The points in Figure 4A are values of Q calculated from the data of Figure 5 using a value of $\bar{k}_c = 0.95 \times 10^7$/s. The agreement between the $Q(T)$ obtained from the static experiments (curve 2 of Figure 4A) and $\bar{\tau}(T)$ (points in Figure 4A) is further evidence that the fatty acid probe remains in the phospholipid through the phase transition.

An interesting aspect of the lifetime measurements is the persistence of a small long lifetime component well above the phase transition (ca. 1% at 50 °C) and a considerable short lifetime component well below the phase transition (30–45% at 25–29 °C). The reality of the small long lifetime component at 50 °C is verified by the fact that the extracted lifetime agrees with the value extrapolated from the lower temperature points (Figure 5A,B). This component may be related to other observations of persistent structural changes above the phase-transition temperature (Lee et al., 1974; Wu and McConnell, 1975). The magnitude of the short-lifetime component at low temperature is very variable and may represent hysteresis. The coexistence of the two lifetime components in the transition region suggests a phospholipid domain structure (Shimshick and McConnell, 1975; Papahadjopoulos et al., 1973; Hui et al., 1974; Blok et al., 1975).

TABLE II: Effect of the DPPC Phase Transition on the *trans*-PnA Absorption Spectrum.

T (°C)	λ_1[a]	α[b]	n	$V(T)/V(20)$[c]
20	321.1	0.300	1.52	1.00
40	319.8	0.289	1.49	1.04
43	318.3	0.274	1.46	1.09
50	318.1	0.270	1.45	1.11

[a] Excitation peak figure. [b] From Figure 2 of Sklar et al. (1977). [c] $V(T)/V(20) = \alpha(20)/\alpha(T)$.

Absorption Spectral Shifts in DPPC Dispersions. The absorption peak position of parinaric acid is a function of the polarizability of the environment. The studies of the previous paper in this issue (Sklar et al., 1977) have shown that the absorption frequency $\bar{\nu}$ is a linear function of $\alpha = (n^2 - 1)/(n^2 + 2)$, where n is the refractive index. Measurements of $\bar{\nu} = 1/\lambda$ may therefore be converted to values of the (effective) refractive index of the medium surrounding the probe. The quantity α is a simple function of the density of the medium. Since there is a density decrease of 4% associated with the phase transition of DPPC (Nagle, 1973; Sheetz and Chan, 1972; Melchior and Morowitz, 1972), there should be a blue shift of the absorption spectrum of parinaric acid of about 1 nm. Conversely, the observed spectral shift may be used to estimate the density decrease.

The absorption peak position of PnA in DPPC vesicles as a function of temperature is shown in Figure 6. The open circles are the peak positions determined from fluorescence excitation spectra, while the filled circles in B are the direct absorption results (Sklar et al., 1976). The observed peak positions are constant with time, indicating that cis–trans isomerization is negligible. The absorption peak values are displaced from the excitation peak values because of the presence of an absorbing but nonfluorescent aqueous component. The fact that the displacement of the absorption peak from the excitation peak is roughly the same below and above the phase transition is further evidence that there is no significant increase in the aqueous component at the transition temperature. An abrupt shift in the peak position of approximately 1.5 nm is observed at the phase transition.

Table II shows the values of the excitation maxima for *trans*-PnA in DPPC at several temperatures and the corresponding values of α obtained from the correlation of $\bar{\nu}$ with α presented in the previous paper of this issue (Sklar et al., 1977). The effective refractive index, $n = [(2\alpha + 1)/(1 - \alpha)]^{1/2}$, is also given. The values obtained with *cis*- and *trans*-PnA are essentially the same and the absolute values obtained are reasonable (Drexhage, 1974; Powers and Clark, 1975). For an isotropic material, α is proportional to the density. The ratio

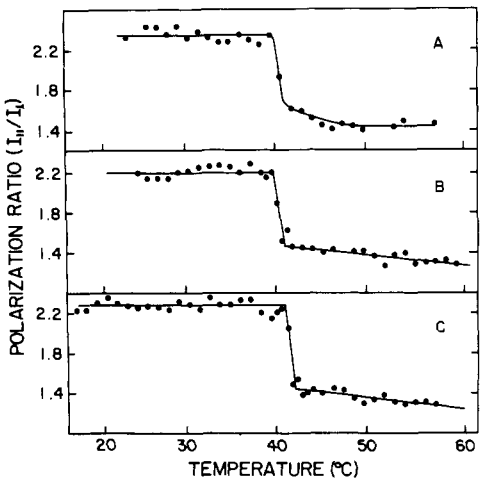

FIGURE 7: The polarization ratio ($I_{\parallel}/I_{\perp}$) for parinaric acid probes in response to the thermal transition of DPPC. (A) Phospholipid derivative of *cis*-PnA in DPPC; (B) *cis*-PnA in DPPC; (C) *trans*-PnA in DPPC. The samples for B and C were those described in Figure 6; the sample for A was prepared as in Figure 4C and contained one 1-palmitoyl-2-*cis*-parinaroylphosphatidylcholine/50 DPPC. Polarization measurements were performed with Glan-Thomson UV polarizers mounted in the fluorimeter. For each sample, temperature, and polarizer orientation, the fluorescence intensity was collected for periods of 15–30 s for a sample and for a lipid-scattering blank. Each data point represents a calculation of $1.1 \times (I_{\parallel}^{S} - I_{\parallel}^{B})/(I_{\perp}^{S} - I_{\perp}^{B})$ where the superscripts S and B refer to sample and blank and the factor of 1.1 represents the measured instrumental preference for horizontal (perpendicular) polarized light. The excitation slits were 20 nm and the emission slits 40 nm.

$\alpha(20\ °C)/\alpha(T)$ is the volume relative to its value at 20 °C, assuming that the effects due to the membrane birefringence can be neglected. The value of $\Delta\rho/\rho$ obtained in this way for a 3 °C range which spans the phase transition temperature is 5.2%. This is in reasonable agreement with the dilatometric value of about 4%.

Fluorescence Polarization of Parinaric Acid Probes in DPPC. Figure 7 shows the polarization ratio $I_{\parallel}/I_{\perp}$ for the parinaroyl phospholipid and *cis*- and *trans*-PnA in DPPC as a function of temperature. The polarization ratio for all of the probes is nearly constant, at a value of at least 2.2, in the temperature range from 20 to 40 °C. No significant change is seen in the pretransition region. At the main transition, the polarization ratio falls to a final value of 1.4 over a width of 2 °C. *cis*-PnA detects the transition about 1 °C lower than *trans*-PnA, as noted previously.

It is not possible to convert these measured polarization ratios to rotational diffusion rates for the probe transition dipole with the available data. It is estimated, however, that the observed polarization decrease corresponds to a change in the rotational diffusion coefficient of at least two orders of magnitude.

The Binding of Parinaric Acid to Phospholipid Vesicles. The fluorescence enhancement associated with the binding of PnA to vesicles saturates at high ratios of probe to lipid (Figure 3). Binding curves were obtained by adding sequential aliquots of PnA to lipid samples and the fluorescence intensity was followed with time until no further increase was observed. The data have been analyzed as a double-reciprocal plot by the methods of Träuble and Overath (1973). This analysis gives an estimate of the minimum number of lipids providing a binding site and the apparent K_d for the binding. Both chain length (DMPC, DPPC, DSPC) and head group (choline, *N*,*N*-dimethylethanolamine, ethanolamine) have been varied (Table III). Temperatures below and above T_c have been studied for each lipid. *trans*-PnA exhibits a lower apparent K_d below T_c than above; in the one lipid studied with *cis*-PnA, the K_d is little changed through the phase transition. This observation is consistent with the notion that *trans*-parinaric acid is preferentially associated with solid-phase lipids, whereas *cis*-parinaric acid distributes between fluid and solid-phase lipids.

TABLE III: Binding of *cis*- and *trans*-PnA to Phospholipids.[a]

Lipid	T (°C)	L/PnA[b]	K_d (μM)[c]	T (°C)	L/PnA[b]	K_d (μM)[c]
DMPC[d]	15	34	0.35	34	30	0.69
DPPC[d]	34	35	0.30	52	20	0.69
DSPC[d]	42	27	0.5	62	14	1.0
DPPE[d]	52	14	1.4	72	9	2.8
Me_2-DPPE[d,e]	40	10	1.4	58	10	1.5
DPPC[f]	32	29	4.1	52	33	5.0

[a] Samples contained 60 nmol of phospholipid in 3.6 mL of 0.01 M phosphate buffer, pH 7.4. The sample was continuously mixed and deoxygenated by bubbling with argon. PnA was added as an ethanol solution with a Hamilton syringe through the top of the sample compartment. Fluorescence binding curves were analyzed as a double-reciprocal plot by the method of Träuble and Overath (1973). [b] Minimum number of lipids providing a "binding site" for PnA. [c] Apparent K_d obtained from double-reciprocal plot. [d] *trans*-PnA. [e] *N*,*N*-Dimethyldipalmitoylphosphatidylethanolamine. [f] *cis*-PnA.

A more appropriate description of the binding of PnA to lipid vesicles is a partition process with a partition coefficient given by

$$K_p = \frac{(\text{moles of probe in lipid/moles of lipid})}{(\text{moles of probe in water/moles of water})} \quad (3)$$

By preparing DPPC dispersions with varying amounts of lipid, and a constant PnA concentration (4×10^{-6} M), centrifuging the lipids and examining the absorption of the supernatant, the amount of parinaric acid in the aqueous phase was determined. The results of this experiment are shown in Figure 8A. The calculated partition coefficient is constant, at a value of $4.7 \pm 0.7 \times 10^5$ up to a lipid/probe ratio of about 25/1. It increases to a value of 10×10^5 at 6/1, which is probably related to complications of fatty acid solubility in the lipid phase.

The absorption spectrum of *cis*-PnA in DPPC dispersions is a function of the lipid concentration, as shown in Figure 9. The aqueous and lipid spectra (Figure 9A and C, respectively) are characterized by distinct absorption maxima (peak 1: 321 and 326 nm, respectively) and low values of the ratio of the optical density at the "valley" to the optical density at "peak 2" (Figure 9A). This extinction ratio is designated V/P. The spectrum of a solution in which there are approximately equal concentrations of the aqueous and lipid species is characterized by an intermediate value of the absorption maximum, and a maximum value of $V/P2$ (Figure 9B). These data are plotted as a function of the lipid/probe ratio in Figure 8B and 8C. It is evident from a comparison of the data of Figure 8A,B,C that the probe is equally distributed between aqueous and lipid phases when the lipid/probe ratio is about 30/1 to 40/1 for a PnA concentration of 4×10^{-6} M.

The free energy of the transfer of *cis*-PnA from aqueous phase to lipid phase is $-RT \ln K_p = -8$ kcal/mol. This is similar to the value obtained for the distribution of stearic acid (−10 kcal) between heptane and water (Smith and Tanford, 1973).

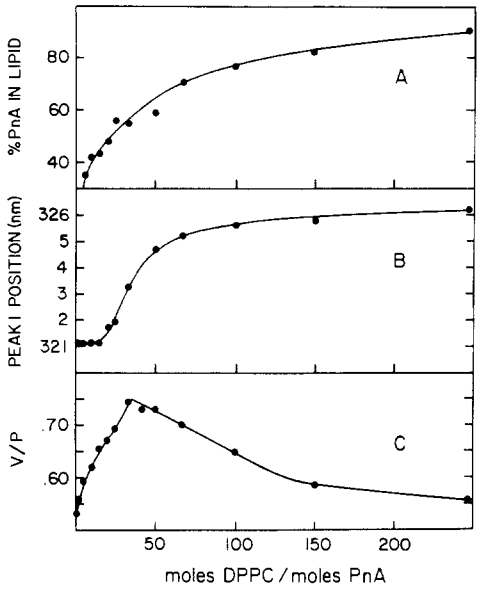

FIGURE 8: The binding of *cis*-PnA to DPPC vesicles at 25 °C. In each case, the concentration of *cis*-PnA was 4×10^{-6} M. (A) The amount bound as determined by the residual aqueous absorption after centrifugation of the lipids (for details, see Sklar (1976)). (B) The position of the longest wavelength absorption maximum. (C) The ratio of the absorption intensity at the longest wavelength minimum ("Valley", see Figure 9) to the intensity of the second absorption maximum ("peak 2", see Figure 9) prior to centrifugation.

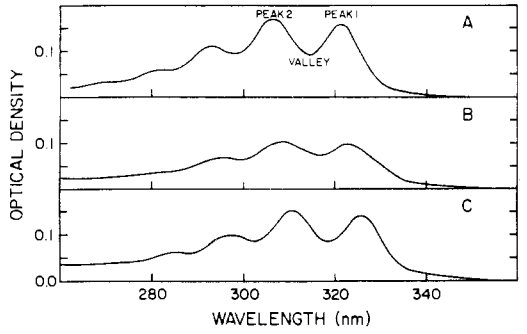

FIGURE 9: The absorption spectra of *cis*-PnA in buffer and lipid. Solutions were prepared as described in the legend to Figure 8. (A) *cis*-PnA in buffer; (B) *cis*-PnA/DPPC in the ratio 33 DPPC/1 PnA; (C) *cis*-PnA/DPPC in the ratio 250 DPPC/1 parinaric acid. All measurements were made prior to centrifugation at 25 °C and the concentration of *cis*-PnA was about 4×10^{-6} M in each case.

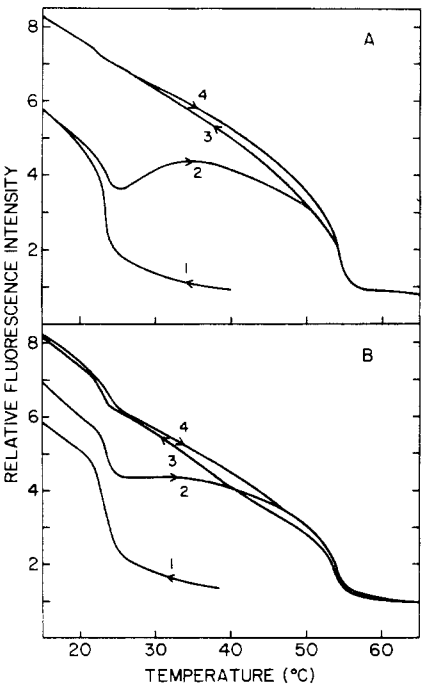

FIGURE 10: The transfer of *trans*-PnA (A) and *cis*-PnA (B) from DMPC to DSPC vesicles. Data are displayed as fluorescence intensity vs. temperature. Dispersions contained 0.05 mg/mL DMPC or DSPC. (A) *trans*-PnA present in DMPC at the ratio of 1 parinaric acid/100 DMPC. (1) cooling curve, DSPC dispersion added in equal volume at 15 °C; (2) heating curve; (3) cooling curve; and (4) heating curve. The fluorescence intensity for cooling curve 1 has been divided by two to compensate for dilution. (B) *cis*-PnA added to DMPC at the ratio of 1 PnA/100 DMPC. Curve identification as for A. Excitation at 320 nm for *trans*- and 325 nm for *cis*-PnA (slit 1.5 nm) with emission at 410 nm (slit 26 nm). Temperature variation was 2 °C/minute.

Kinetics of Parinaric Acid Uptake by Phospholipid Vesicles. The rate of uptake *trans*-PnA by phospholipid vesicles varies extensively with the temperature, the probe/phospholipid ratio and the type of phospholipid dispersion. When *trans*-PnA is added to a multilamellar dispersion of DPPC (prepared by vortexing) at the low ratio of 1 *trans*-PnA to 300 DPPC, the uptake is rapid (with a half-time less than 30 s) at temperatures above or below T_c. However, when the ratio is high, 1 *trans*-PnA to 3 DPPC, the uptake is rapid above T_c, but clearly biphasic below T_c with a slow process estimated to have a half-time of 6 min. Uptake by these multilamellar dispersions involves at least two processes after binding by the outermost monolayer. These are the "flip-flop" from outer to inner monolayer of the outermost bilayer and subsequent transfer across an aqueous compartment to inner lamellae. The uptake of high ratios of *trans*-PnA by single-walled vesicles (prepared by sonication) below T_c is rapid and monophasic. Our results suggest that fatty acid "flip-flop" is rapid, while the transfer steps are slow, at least under these conditions.

trans-Parinaric Acid Accumulates in Solid Phases; cis-Parinaric Acid Distributes between Coexisting Fluid and Solid Phases. The distribution of *cis*- and *trans*-PnA between coexisting fluid and solid vesicles was determined as shown in Figure 10. *trans*-PnA was added to DMPC above its phase-transition temperature at a probe/lipid ratio of 1/100. When the temperature was lowered (curve 1, Figure 10A), the characteristic DMPC transition is observed. An equal volume of DSPC vesicles was added to the DMPC vesicles at 15 °C. When the temperature was increased (curve 2), the DMPC transition is observed but diminished in magnitude, and the DSPC transition was observed. When the temperature was lowered (curve 3), the DSPC transition remains, but only a trace of the DMPC transition was observed. Upon heating (curve 4), the DSPC transition remains. The probe has transferred from DMPC to DSPC in curve 2 as the DMPC melts and remains associated with the higher melting component. The decrease in magnitude of the DMPC transition in curve 2 represents rapid partial transfer of PnA to DSPC. The subsequent increase in intensity between 25 and 40 °C represents slow-transfer steps (perhaps limited by uptake and transfer to inner DSPC compartments).

Identical experiments were performed with *cis*-PnA (Figure 10B). *cis*-PnA distributes between phases, and, after the partition equilibrium has been established, it detects both transitions (curves 3 and 4 of Figure 10B). In a similar study with DPPC and dielaidoylphosphatidylcholine (DEPC, prepared by the method of Baer and Buchnea, 1959), *trans*-PnA

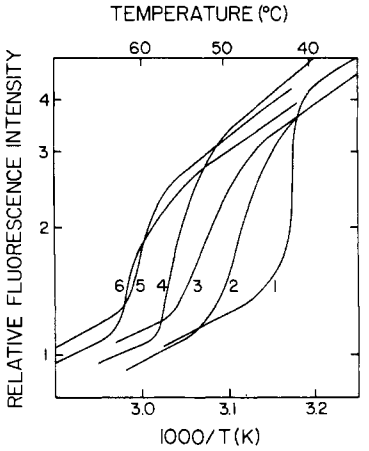

FIGURE 11: Fluorescence of *trans*-PnA in DPPC–DPPE mixtures (cooling curves). Log (I) vs. $1/T$. The numbers designate increasing mol % of DPPE: (1) 0%, (2), 21%, (3) 42%, (4) 62%, (5) 81%, (6) 100%. The lipids were codeposited and dispersed by vortexing at 70 °C to produce suspensions containing 0.05 mg/mL total lipid, 1 BHT/100 lipids and 1 *trans*-PnA/100 lipids. Fluorescence excitation: 322 nm, 1.5-nm slits; emission: 410 nm, 16-nm slits.

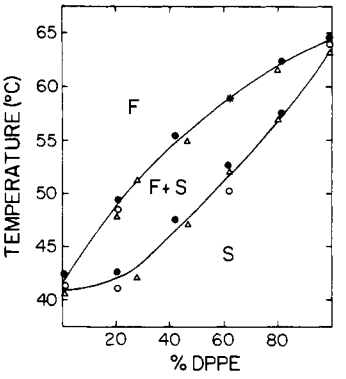

FIGURE 12: The DPPC/DPPE phase diagram. (●) *trans*-PnA; (○) *cis*-PnA; (△) Tempo data of Shimshick and McConnell (1973). The asterisk represents three coincident data points.

transfers quantitatively to the higher melting lipid, DPPC. DEPC has a melting point of 11 °C (Wu and McConnell, 1975). Thus, the partition coefficient between lipid types seems to be dominated by the lipid fluidity, rather than the chain length. To our knowledge, there is no report of any other probe molecule that concentrates in lipid solid phases. When similar experiments are performed with spin-labeled fatty acids, they are shown to transfer to fluid lipids (Butler et al., 1974). Likewise, a number of fluorescence-labeled fatty acids partition preferentially into the more fluid phase (Bashford et al., 1976).

At high *trans*-PnA to lipid ratios, it is possible to observe the transitions of both the high- and low-melting components. At high levels of PnA, the binding to the solid phase saturates and the probe then accumulates in fluid-phase lipids. These results may be put on a quantitative basis so that the mole fraction of the *trans*-PnA in each phase can be determined from the magnitude of the fluorescence changes at each transition (Sklar, 1976). Analysis of the data in Figures 4 and 10 indicates that *cis*-PnA distributes equally between solid and fluid phases while *trans*-PnA has a partition coefficient of about 3, distributing preferentially into the solid phase.

The DPPC/DPPE Phase Diagram. For two-component lipid mixtures, the lateral-phase separation behavior is most conveniently represented as a phase diagram (Shimshick and McConnell, 1973). The onset and completion of the lateral-phase separation are identified as breaks in the temperature dependence of a property which is characteristic of the lipid state. The DPPC/DPPE phase diagram has been chosen for initial investigation of the utility of PnA fluorescence in this application. Figure 11 shows the fluorescence intensity data obtained with *trans*-PnA for lipid mixtures containing 0, 21, 42, 62, 81, and 100% DPPE. The breakpoints are identified as the solidus and liquidus temperatures, and the corresponding phase diagram is given in Figure 12. The solid circles are the *trans*-PnA results, the open circles are for *cis*-PnA, and the triangles are the Tempo data of Shimshick and McConnell (1973). For any one composition, the difference in the solidus or liquidus temperature detected by the probes is approximately equal to the combined uncertainty of the measurements. However, the *trans*-PnA points are consistently higher than the *cis*-PnA or Tempo points, presumably due to preferential accumulation of the trans probe in solid-phase regions. Basically, however, the agreement between the results for the two techniques is excellent.

Summary and Conclusions

The parinaric acid probes are naturally occurring fatty acids which strongly resemble lipid components of biological membranes (Sklar et al., 1975). The spectroscopy of these molecules has been studied in detail and the spectral response of these molecules to their environment is reasonably well understood (Sklar et al., 1977). Several spectral properties of the parinaryl chromophore make it a useful fluorescence probe. In particular, the absorption near 320 nm is very strong, the fluorescence quantum yield in solid-phase lipids is high (ca. 0.3), while in water the quantum yield is negligible. The emission does not overlap the absorption.

A variety of spectral properties of parinaric acid are responsive to changes in the physical structure of the lipid environment. (a) Lipid-phase transitions are marked by a two- to fourfold change in the fluorescence quantum yield and lifetime. (b) Two fluorescence lifetimes are easily resolved which are associated with fluid and solid-phase lipids. (c) The absorption peak position shifts about 1.5 nm in response to the DPPC transition, reflecting a 5% bilayer expansion. (d) The polarization of fluorescence changes abruptly at the transition, indicating a change in the rotational diffusion coefficient of two orders of magnitude.

A number of features of lipid–parinaric acid interactions further enhance the utility of these probes. (a) Equilibration of the distribution of the added probe is rapid at temperatures above the phase transition. (b) The amount of probe in the aqueous phase does not change appreciably at a lipid-phase transition. (c) The fluorescence changes are generally highly reversible in the absence of free radicals and oxygen. (d) The observed spectral changes at a phase transition are as sharp as those reported with any physical technique for the same type of lipid dispersion. (e) Only minor perturbations of the observed transitions occur even at the level of 1 probe/30 lipid molecules. (f) The trans probe preferentially partitions into solid-phase lipids in contrast to the behavior of many other probes (including *cis*-parinaric acid) but the magnitude of this preferential partitioning has only a small effect on observed transition temperatures.

Another important aspect of the use of parinaric acid as a membrane probe is that it is available in large quantities (see Materials and Methods) for biosynthetic (Tecoma et al., 1977) or synthetic procedures. The carboxylic acid functional group can be transformed without destruction or even isomerization

of the polyene chromophore. The preparation of methyl esters, mixed anhydrides, and phosphatidylcholines are described above and the acid chloride and isocyanate have also been prepared.

The geometric similarity of parinaric acid to the corresponding saturated or monounsaturated acyl chains of lipids has been discussed elsewhere (Sklar et al., 1975), where it was pointed out that the length of the polyene chain is identical to that of a saturated chain because of compensating differences in both bond lengths and bond angles. Biosynthetic incorporation experiments described in the following paper of this issue (Tecoma et al., 1977) demonstrate the lack of significant perturbation of biological membrane functions. The fluorescence studies presented here demonstrate the lack of significant perturbation of the physical properties of lipid bilayers. The spectroscopic studies of the previous paper in this issue (Sklar et al., 1977) and of linear polyenes in general (Hudson and Kohler, 1974) provide a significantly greater level of understanding of the spectral response of parinaric acid to its environment than that which is available for any other fluorescent membrane probe.

Acknowledgments

We acknowledge the assistance of Stuart Bursten in the partitioning and binding experiments, Daniel Graham in the investigation of phospholipid synthetic methods, and Marianne Petersen in the preparation of *trans*-parinaric acid, and helpful discussions with Prof. Edward Dratz concerning the use of BHT and argon as antioxidants, and Dr. W. Stone concerning fatty acid binding to phospholipid dispersions. We thank Prof. Lubert Stryer for the use of his fluorescence lifetime apparatus, Dr. W. Veatch for help in the lifetime measurements, and Carolyn Kobielus and Diane Simoni for assistance in the preparation of this manuscript.

References

Backer, C. A., and Bakhuizen Van den Brink, R. C., Jr. (1963), Flora of Java, Noordhoff, Groningen, The Netherlands, p 522.

Baer, E., and Buchnea, D. (1959), *Can. J. Biochem. Physiol. 37,* 953.

Bartlett, G. R. (1959), *J. Biol. Chem. 234,* 466.

Bashford, C. L., Morgan, C. G., and Radda, G. K. (1976), *Biochim. Biophys. Acta 426,* 157.

Blok, M. C., Van Der Neut-Kok, E. C. M., Van Deenen, L. L. M., and De Gier, J. (1975), *Biochim. Biophys. Acta 406,* 187.

Butler, K. W., Tattrie, N. H., and Smith, I. C. P. (1974), *Biochim. Biophys. Acta 363,* 351.

Drexhage, K. H. (1974), *Prog. Opt. 12,* 174.

Eckey, E. W. (1954), Vegetable Fats and Oils, New York, N.Y., Reinhold, p 470.

Gunstone, F. D., and Subbarao, R. (1967), *Chem. Phys. Lipids 1,* 349.

Hanahan, D. J. (1952), *J. Biol. Chem. 195,* 199.

Hinz, H. J., and Sturtevant, J. M. (1972), *J. Biol. Chem. 247,* 6071.

Hopkins, C. Y. (1972), *Top. Lipid Chem. 3,* 37.

Hubbell, W. L., and McConnell, H. M. (1971), *J. Am. Chem. Soc. 93,* 314.

Hudson, B., and Kohler, B. (1974), *Annu. Rev. Phys. Chem. 25,* 437.

Hui, S. W., Parsons, D. F., and Cowden, M. (1974), *Proc. Natl. Acad. Sci. U.S.A. 71,* 5068.

Jacobson, K., and Papahadjopoulos, D. (1975), *Biochemistry 14,* 152.

Kaufmann, H. P., and Sud, R. K. (1959), *Chem. Ber. 92,* 2797.

Kraemer, J. H. (1951), Trees of the Western Pacific Region, West Lafayette, Indiana, p 107.

Lee, A. G., Birdsall, N. J. M., Metcalfe, J. C., Toon, P. A., and Warren, G. B. (1974), *Biochemistry 13,* 3699.

Melchior, D. L., and Morowitz, H. J. (1972), *Biochemistry 11,* 4558.

Nagle, J. F. (1973), *Proc. Natl. Acad. Sci. U.S.A. 70,* 3443.

Papahadjopoulos, D., Jacobson, K., Nir, S., and Isac, T. (1973), *Biochim. Biophys. Acta 311,* 330.

Peifer, J. T. (1962), *Mikrochim. Acta* 529.

Powers, L., and Clark, N. A. (1975), *Proc. Natl. Acad. Sci. U.S.A. 72,* 840.

Riley, J. P. (1950), *J. Chem. Soc.,* 12.

Robles, E. C., and Van den Berg, D. (1969), *Biochim. Biophys. Acta 187,* 520.

Sheetz, M. P., and Chan, S. I. (1972), *Biochemistry 11,* 4573.

Shimshick, E. J., and McConnell, H. M. (1973), *Biochemistry 12,* 2351.

Sklar, L. A. (1976), Thesis, Stanford University.

Sklar, L. A., Hudson, B. S., Peterson, M., and Diamond, J. (1977), *Biochemistry 16* (first in a series of three in this issue).

Sklar, L. A., Hudson, B. S., and Simoni, R. D. (1975), *Proc. Natl. Acad. Sci. U.S.A. 72,* 1649.

Sklar, L. A., Hudson, B. S., and Simoni, R. D. (1976), *J. Supramol. Struct. 4,* 449.

Smith, R., and Tanford, C. (1973), *Proc. Natl. Acad. Sci. U.S.A. 70,* 289.

Solodovnik, V. D. (1967), *Russ. Chem. Rev. (Engl. Transl.) 36,* 272.

Tecoma, E., Sklar, L. A., Simoni, R. D., and Hudson, B. S. (1977), *Biochemistry 16* (third in a series of three in this issue).

Träuble, H., and Overath, P. (1973), *Biochim. Biophys. Acta 307,* 491.

Wu, S. H., and McConnell, H. M. (1975), *Biochemistry 14,* 847.

Yguerabide, J. (1972), *Methods Enzymol. 26,* 498.